ELSEVIER

Ultrasonics 40 (2002) 49–54

Ultrasonics

www.elsevier.com/locate/ultras

Evaluation of the contact resonance frequencies in atomic force microscopy as a method for surface characterisation (invited)

U. Rabe *, M. Kopycinska, S. Hirsekorn, W. Arnold

Fraunhofer Institute for Nondestructive Testing (IZFP), Bldg. 37, University, D-66123 Saarbrücken, Germany

Abstract

The combination of ultrasound with atomic force microscopy (AFM) opens the high lateral resolution of scanning probe techniques in the nanometer range to ultrasonics. One possible method is to observe the resonance frequencies of the AFM sensors under different tip–sample interaction conditions. AFM sensors can be regarded as small flexible beams. Their lowest flexural and torsional resonance frequencies are usually found to be in a range between several kHz and several MHz depending on their exact geometrical shape. When the sensor tip is in a repulsive elastic contact with a sample surface, the local indentation modulus can be determined by the contact resonance technique. Contact resonances in the ultrasonic frequency range can also be used to improve the image contrast in other dynamic techniques as, for example, in the so-called piezo-mode. Here, an alternating electric field is applied between a conducting cantilever and a piezoelectric sample. Via the inverse piezoelectric effect, the sample surface is set into vibration. This excitation is localised around the contact area formed by the sensor tip and the sample surface. We show applications of the contact resonance technique to piezoelectric ceramics. © 2002 Elsevier Science B.V. All rights reserved.

Keywords: Atomic force microscopy; Dynamic modes; Ultrasound; Elasticity; Contact mechanics; Contact stiffness; Contact resonance; Nanoindentation

1. Introduction

Atomic force acoustic microscopy (AFAM) [1–5] can be considered as a near-field acoustic [6] technique or as a special operational mode of atomic force microscopy (AFM). As in another dynamic AFM technique such as the tapping mode [7], the cantilever is vibrating in one of its resonance frequencies as it is scanned across the sample surface. Different types of vibrations, mainly flexural and torsional modes, are possible for the cantilevers. Typical dimensions of micro-fabricated AFM cantilevers are several 100 μm's length, several 10 μm's width, and several μm thickness. The resulting lowest resonance frequencies range from several kHz up to several 100 kHz. In dynamic AFM, the cantilever is often modeled as a simple harmonic oscillator vibrating only in its lowest resonance frequency. Stiffer cantilever beams vibrating at frequencies above 50 kHz are sometimes preferred. The operating frequencies of the dynamic AFM may therefore be in the ultrasonic range. In contrast to the AFAM however, the dynamic AFM is generally not thought of as an ultrasonic technique.

2. Principle of AFAM and contact resonance spectroscopy

The principle of AFAM and contact resonance spectroscopy is shown schematically in Fig. 1. The cantilever is described as a small flexural beam with a defined infinite set of resonance frequencies. If the sensor tip is not in contact with a sample surface, the situation of a clamped-free beam arises which is treated in mechanics textbooks (e.g. [8]). When the tip is brought close to a sample surface the mutual interaction forces modify the mechanical boundary conditions at the cantilever end to no longer be free. The tip–sample forces are a non-linear function of distance and are attractive at larger distances. In contact, the interaction becomes repulsive when the tip is pressed into the sample. Though in principle all types of forces can be measured by AFAM, the purpose here is to measure surface elastic forces. Therefore, the tip is in direct contact with the sample

* Corresponding author. Tel.: +49-681-9302-3863; fax: +49-681-9302-5903.

E-mail address: rabe@izfp.fhg.de (U. Rabe).

0041-624X/02/$ - see front matter © 2002 Elsevier Science B.V. All rights reserved.
PII: S0041-624X(02)00089-6

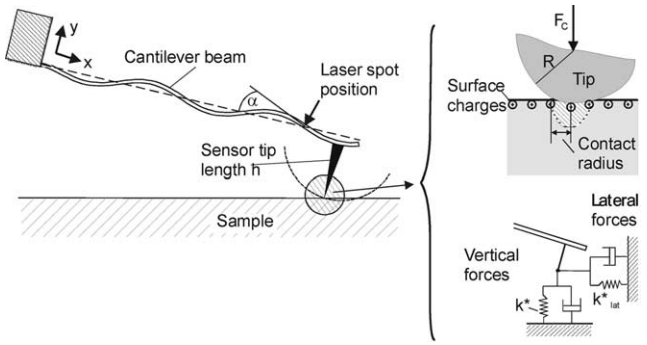

Fig. 1. Principle of AFM contact resonance spectroscopy. The AFM cantilever can be described as a flexural beam with a clamped end. The boundary conditions at the other end are given by the tip–sample interaction forces. In contact, repulsive elastic forces as well as electrical forces due to surface charges play a major role. These forces can be approximated by linear spring-dashpot systems if the vibration amplitudes remain small.

surface. The static load applied by the cantilever is chosen to be high enough (several 100 nN) to ensure predominance of elasticity effects and allow the neglect of adhesion. To a first approximation, the repulsive part of the force curve is well described by the Hertz model [9]. The radius of the contact area ranges between several nm's and several 10 nm's. It depends on the applied static force, the radius of the sensor tip, and the elastic constants of the tip and the surface.

When non-linear forces such as those listed above form the boundary condition at the unclamped end of the cantilever, the equation of motion must be solved at least partially numerically [10–12]. For small tip–sample vibration amplitudes, however, the forces can be approximated linearly, i.e. the non-linear forces can be replaced by linear springs. The characteristic equation of a flexural beam confined by a set of springs and dashpots can be calculated analytically. It is then easily seen that a spring-coupled end leads to a new set of resonance frequencies of the beam, each shifted with respect to the corresponding free resonance. Generally, these shifts are considerable when the tip approaches a sample surface, so that the contact resonance frequencies appear in a quite different frequency range than the corresponding free resonances. The frequency shifts depend on the stiffness of the spring, called the contact stiffness k^*. Therefore, the contact stiffness can be calculated from measured contact resonance frequencies of the cantilever beam when certain properties of the beam are known. This is the basic principle of AFM contact resonance spectroscopy. Because the characteristics of the beam are often not known precisely, when quantitative results are sought it is better to measure more than one contact resonance frequency as well as the free resonances. Parameters in the theoretical model such as the precise position of the sensor tip position along the length axis of the beam can then be fit.

When the vibration amplitudes are small, such that the resonance peaks show a linear behavior with excitations, the contact resonance frequencies are directly related to the contact stiffness, assuming that the vibration modes of the beam are known precisely. In a second step, the contact stiffness is related to a surface property, here the elasticity of the surface layer of the sample. A realistic tip–sample force model must be assumed and further input parameters such as the radius of the sensor tip are required. To provide these data, we currently measure resonance spectra on a reference sample, whose elastic constants are known, before and after the measurements on the unknown sample. In this way, the missing parameters, especially the tip geometry can be approximated. A more detailed description of the procedures is given in [13].

Images can also be collected in the AFAM mode. A contact resonance frequency is measured by a frequency scan. Then a frequency close to this resonance is chosen as fixed excitation frequency and the cantilever vibration amplitude or its phase is monitored while the sample surface is scanned. An example is shown in Fig. 2. The sample was a bulk lead zirconate–titanate (PZT) ceramic (PIC 151 [14]) as used for ultrasonic transducers. A thin slice of less than 1 mm thickness was cut from a larger piece and one surface was carefully polished. The can-

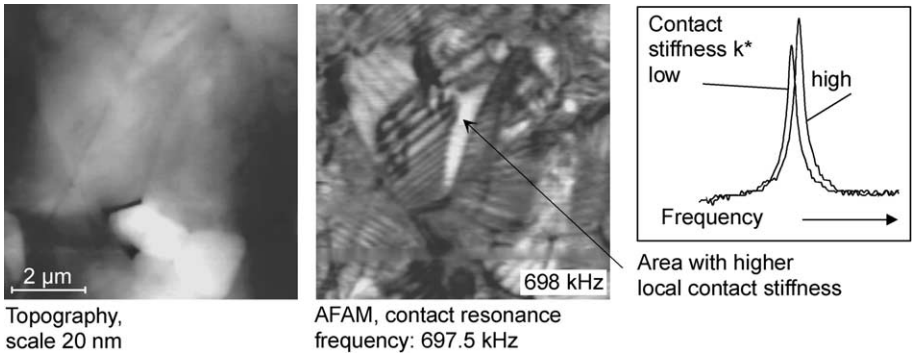

Fig. 2. Topography (left) and AFAM amplitude image (middle) of a polished bulk ferroelectric ceramic. The AFAM image was taken at a frequency above the contact resonance. In the contact spectra (right), areas of high contact stiffness appear brighter than those of lower contact stiffness.

tilever and the sample were electronically grounded in order to avoid electrostatic charging. The topographic image which was simultaneously acquired with the AFAM amplitude image shows the grains in the ceramic which form plateaus of different height. The AFAM image reveals a substructure within the grains indicating variations in contact stiffness. From comparison to images recorded by well-known techniques such as etching followed by REM imaging these are identified as ferroelectric domain structures. If a frequency higher than the contact resonance is chosen as excitation frequency, areas of high contact stiffness appear brighter than those of lower contact stiffness (as in Fig. 2). An excitation frequency below the contact resonance leads to a contrast inversion.

3. Experiments

In order to examine the ultrasonic contrast in AFAM images, we observed the shift of the contact resonance frequency on individual scan lines of a PZT sample. To do so, we scanned slowly and stored a spectrum at each data point. From these spectra, we estimated the upper and lower limits of elastic constants of the sample surface. The crystal lattice of PZT has a cubic Perovskite structure. Below the Curie temperature ($T_C = 386$ °C for PIC 151 [14]) the lattice deforms spontaneously into a tetragonal or rhomboedric shape resulting in a spontaneous electrical polarization [15]. Ferroelectric domains of equal polarization result such that the internal energy of the crystal is minimum. The dimensions of the domains are of the same order of magnitude or larger than the contact area between the tip and sample surface. Therefore, the AFM tip effectively probes individual, small, polarized single crystals within the polycrystalline ensemble. The contrast in AFAM results from the variation in effective stiffness between different domains. In ferroelectrics an important contribution to the effective forces is from the electrical polarization.

Macroscopically, piezoelectric stiffening is well known [15,16]. Young's modulus $Y_3^{D,E} = 1/s_{11}^{D,E}$ of a polarized polycrystal measured parallel (in the 3-direction) is higher than $Y_1^{D,E} = 1/s_{11}^{D,E}$ measured perpendicular to the electrical polarization vector (in the 1-direction). Here, $s_{ij}^{D,E}$ are the compliance constants of the material, the superscripts E and D represent the constant electric field and the constant electric displacement, respectively. The calculated numerical results for PIC 151 using the macroscopic elasticity data given in [14] are $Y_1^E = 60$ GPa, $Y_3^E = 52.6$ GPa, $Y_1^D = 70.0$ GPa, $Y_3^D = 118.76$ GPa. In agreement with theory we found that the macroscopic longitudinal sound velocity of our PZT samples was generally higher in 3-direction than in 1-direction [17]. Single crystal data are not available for PZT. Therefore, the macroscopic data can only provide a rough estimate for the AFM measurement results.

Although the AFM tips and cantilevers employed in the present study were doped and therefore electrically conductive, the variation of Young's moduli obtained from our contact resonance experiments corresponds to the anisotropy expected in the case of constant electric displacement D. The mechanical stress field caused by the AFM tip in the sample is inhomogeneous and decays within a thin surface layer approximately three times the contact radius. Obviously, the local change in the polarization field within the compressed volume cannot be compensated for by a charge transfer between the tip and a counter electrode on the opposite side of the sample. Hence, this polarization field causes an additional restoring force which leads to higher stiffness constants and to considerable elastic anisotropy.

When interpreting the contrast on PZT samples, the extremely high pressure in the contact area must be considered which may lead to a local alteration of the piezoelectric constants. If for example in a typical experiment a force of 840 nN is applied by deflecting a cantilever with a spring constant of 42 N/m by 20 nm, the pressure would be 670 GPa for a contact radius of 20 nm and 54 GPa for a contact radius of 50 nm, respectively. Macroscopic experiments show that the piezoelectric coefficients of PZT change with compressive stress. Typically, compressive stresses between 70 and 100 MPa can result in an increase or a decrease of the piezoelectric coefficients of up to 50% depending on the exact composition and dopand concentration of the material [18].

To probe the non-linear force curve in an AFAM experiment, either the static cantilever force or the ultrasonic excitation amplitude can be varied. A PZT sample and a silicon single crystal with (1 0 0)-surface as a reference sample were each coupled to a commercial ultrasonic transducer. The AFAM contact resonance spectra were measured as a function of the surface vibration amplitude (Fig. 3). As can be seen in Fig. 3 contact resonance frequencies on the silicon and the PZT samples are quite close to each other. After the AFAM measurements, the absolute surface vibration amplitude was measured as a function of electrical excitation using an optical interferometer. Both samples were examined at the relevant frequencies close to their first and second contact resonance frequencies, 750 and 2170 kHz, respectively. These calibration functions yield the absolute surface vibration amplitudes in the AFAM experiments. Furthermore, the beam deflection position detector of the AFM was calibrated. A beam deflection sensor measures the slope, $\alpha = dy/dx$, of the cantilever at the position where the laser spot is focused, as shown schematically in Fig. 1. The relation between cantilever deflection and slope depends on where the laser spot is focused, the flexural wavelength, and the position of the vibration nodes. Therefore, not only the contact stiffness

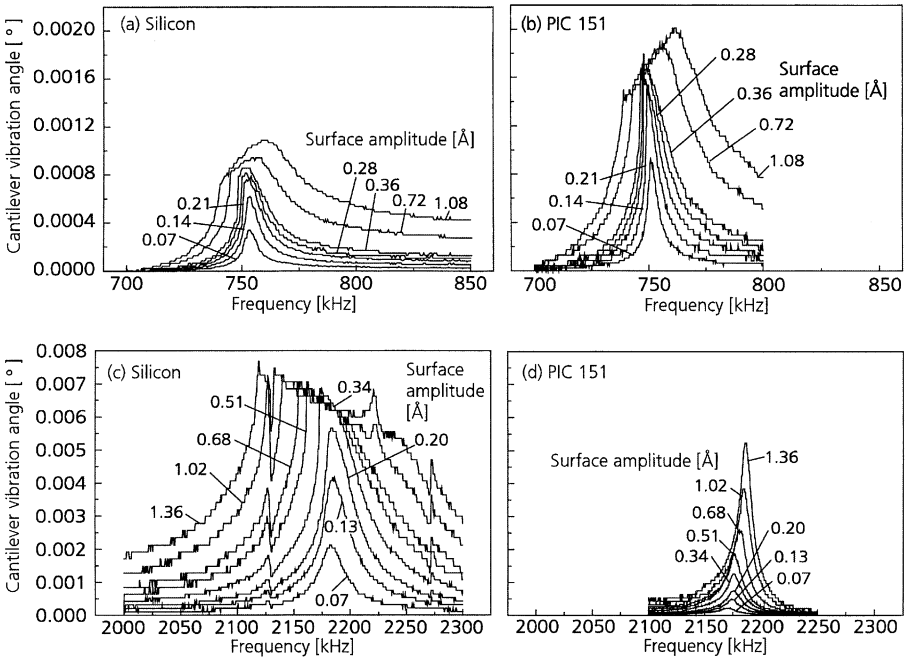

Fig. 3. Contact resonance spectra at different ultrasonic excitation amplitudes on a silicon reference sample and on PZT. The cantilever vibration angle displayed on the vertical axis of the spectra is the dynamic slope α measured by the beam deflection detector and calibrated as described in the text. The first (a and b) and the second flexural mode (c and d) of a silicon cantilever were measured. The free resonance frequencies of the cantilever were 276.84 and 1532.22 kHz, respectively. The cantilever spring constant was 42 N/m.

but also the vibration mode has an influence. In a quasi-static experiment, the slope α is related to the deflection y at the end of the beam by $\alpha = 1.5y/L$ [8,19], where L is the length of the cantilever. Using this relation, the angular sensitivity of the detection unit can be calibrated with a quasi-static force–calibration curve, leading to the calibration of the vertical axis of the spectra in angular units. The calibrated output of the beam deflection detector is called cantilever vibration angle.

For small excitation amplitudes, the resonance peaks in Fig. 3 are symmetric as to be expected from a linearly approximated force curve. When the amplitude is increased, the maxima of the spectra on silicon shift to lower frequencies, the spectra become asymmetric, and a steep frequency jump develops on the left side of the maximum. This is the behavior of a softening resonance as is expected from a tip–sample force curve consisting of a elastically repulsive Herzt'ian force and a long-range attractive force [12]. On PZT for the same surface vibration amplitudes the oscillation behavior of the cantilever is quite different. The resonance spectra are sharper, i.e. the quality factor is higher and the resonance maximum does not shift as much to the left as on silicon. The second resonance frequency even increases with excitation amplitude as shown in Fig. 4. This is a clear deviation from the behavior one would expect in a purely elastic and adhesive contact.

In the AFAM technique described so far, the cantilever vibration is excited with a bulk transducer below the sample. The waves propagate through the sample and cause an out-of-plane vibration of the upper sample surface. At the ultrasonic frequencies used, 750 and 2170 kHz, the acoustic wavelength of the longitudinal waves in PZT is 5.3 and 1.8 mm, respectively, calculated with a longitudinal sound velocity in PZT of 4 mm/μs. It is inherent in near-field techniques that the wavelength of the signal is much larger than the linear dimensions of the receiving or emitting object, here the contact radius of the tip. Here, the wavelength is even orders of magnitude larger than the scan size (typical values are 5×5–

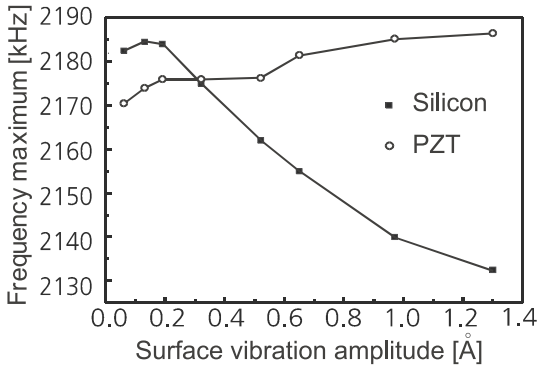

Fig. 4. Shift of the resonance frequency of the second flexural mode as a function of sample surface vibration amplitude. While on silicon a softening is observed, the resonance frequency on PZT slightly increases with increasing excitation amplitude.

$20 \times 20\ \mu m^2$). Therefore, one can assume that the surface vibrates with constant amplitude within the scanned area even if there might be acoustic interference in the sample.

The samples examined here are piezoelectric themselves and therefore convenient to be investigated by the so-called piezo-mode [20,21]. This method uses an electrically conductive sensor tip as a local electrode. An excitation voltage is applied between the tip and a counter-electrode at the back-side of the sample. The local electric field of the tip causes a surface displacement via the inverse piezoelectric effect. The phase and direction of the surface displacements depend on the polarization direction of the probed domain. Fig. 5 shows a schematic diagram of the piezo-mode technique in comparison to the acoustic mode.

In the conventional piezo-mode a fixed excitation frequency (20 kHz) below the first resonance of the cantilever beam is applied. Labardi et al. [22] found different resonance peaks on triglycine sulfate (TGS) at frequencies above the first free resonance and used them for contrast enhancement in piezo-mode imaging. We used the piezo-mode to excite contact resonances of the cantilever on the PZT sample. As can be seen in Fig. 6, the resonances obtained in this ultrasonic piezo-mode are very close to the AFAM contact resonances. As in AFAM, they can be called contact resonances because they disappear when the sensor tip looses contact with the sample surface. In contrast to AFAM, the piezo-mode contact resonances shift only slightly when the excitation amplitude is increased. In piezo-mode linescans, the cantilever vibration amplitude at resonance varies from domain to domain. The resonance frequency, however, varies less than in the acoustic mode. Furthermore, in our experiments so far, the piezo-mode resonance frequencies are higher than the corresponding AFAM contact resonances even though the same cantilever and the same static loads were used. Obviously, an additional static force acts in piezo-mode. For the lowest amplitude spectra in Fig. 6 which were obtained with 0.07 Å excitation amplitude in the AFAM mode, and with 1 V excitation in the piezo-mode, the difference amounts to 36 kHz. When the applied static cantilever force was increased from 420 to 840 nN, a frequency shift of 15 kHz was observed on silicon using the same flexural mode of this cantilever. We therefore conclude that the additional static force in the ultrasonic piezo-mode must be several 100 nN or more.

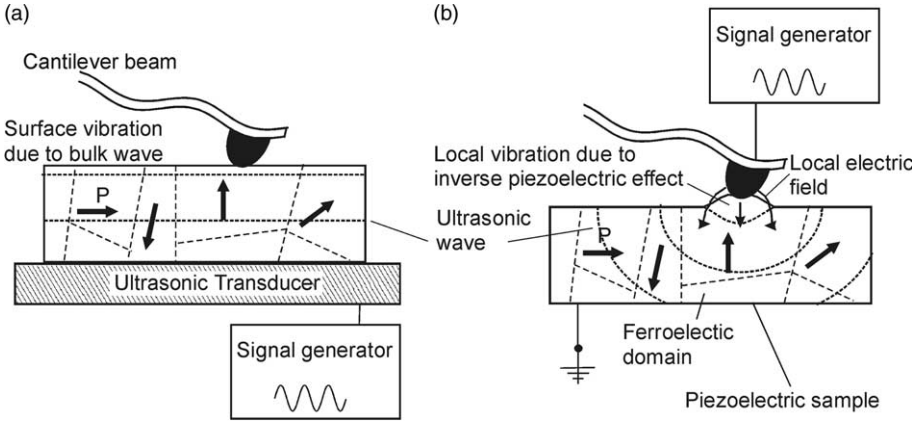

Fig. 5. When the sample is piezoelectric, contact resonance vibrations of the AFM sensor can be excited either with an ultrasonic transducer below the sample (a, acoustic mode) or by a local electric field applied to the sensor tip (b, piezo-mode).

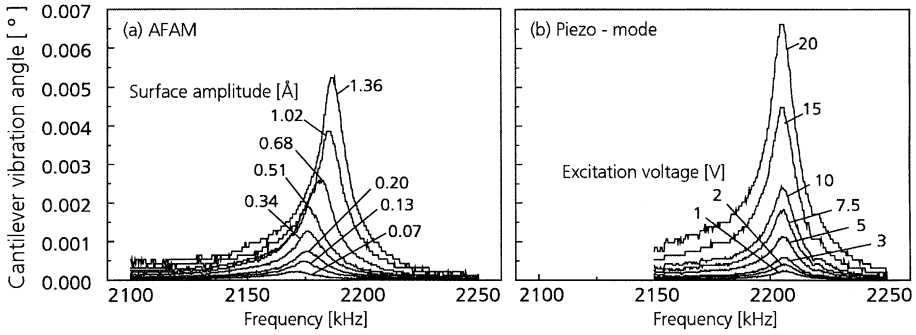

Fig. 6. Vibration spectra of a silicon cantilever (spring constant of 42 N/m) on a PIC 151 sample under a static load of 420 nN and excited by an ultrasonic transducer below the sample (a, AFAM) and by an electric voltage at the sensor tip (b, piezo-mode), respectively.

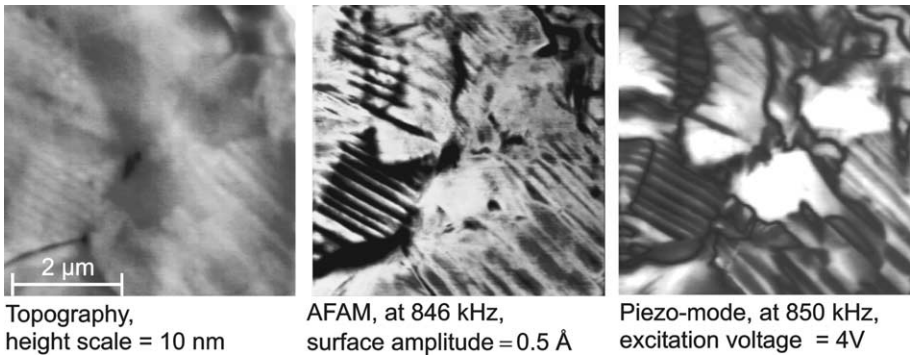

Fig. 7. Topography, acoustic mode amplitude, and piezo-mode amplitude images of a PZT ceramic surface. The excitation frequencies in the dynamic modes are chosen to be near to the first contact resonance of the cantilever. Both dynamic techniques are capable of imaging not only the different grains but also the substructures within the grains due to ferroelectric domains of different polarization.

Comparison of the deflection amplitudes in AFAM and in piezo-mode (Figs. 6(a) and (b)) shows, that an excitation voltage of 15–20 V in the piezo-mode generates the same cantilever vibration amplitude as an acoustic surface vibration amplitude of 1.36 Å. Fig. 7 shows the topography, an acoustic mode amplitude, and a piezo-mode amplitude image of a PZT ceramic surface. The excitation frequencies in the dynamic modes are chosen close to the first contact resonance of the cantilever. In contrast to the topography image, both dynamic techniques were capable of imaging not only the different grains but also substructures within these grains because of ferroelectric domains of different polarization.

4. Conclusion

We showed that AFM cantilever contact resonance vibrations can be excited on PZT ceramics via the local piezoelectric effect. The contact resonance frequencies obtained in this way are higher than the corresponding resonance frequencies in the acoustic mode. Piezo-mode images can be collected using a contact resonance frequency as the excitation frequency while a sample surface is scanned. The choice of contact resonances leads to a contrast enhancement in piezo-mode imaging.

Acknowledgements

We thank D.C. Lupascu and J. Rödel, Technical University of Darmstadt, Germany, for many helpful discussions on piezoelectric ceramics. This work was financially supported by the German Science Foundation within the research program "Multifunctional Materials". M.K. was supported by the "Sonderforschungsbereich 277" at the University of the Saarland, Saarbrücken, Germany. One of the authors (S.H.) thanks also the Volkswagen Foundation for financial support.

References

[1] U. Rabe, K. Janser, W. Arnold, Rev. Sci. Instrum. 67 (1996) 3281.
[2] P.E. Mazeran, J.L. Loubet, Tribol. Lett. 3 (1995) 125.
[3] O. Wright, N. Nishiguchi, Appl. Phys. Lett. 71 (1997) 626.
[4] K. Yamanaka, S. Nakano, Appl. Phys. A 66 (1998) S313.
[5] N.A. Burnham, G. Gremaud, A.J. Kulik, P.J. Gallo, F. Oulevy, J. Vac. Sci. Technol. B 14 (1996) 1308.
[6] J.K. Zieniuk, A. Latuszek, in: H. Shimizu, N. Chubachi, J. Kushibiki (Eds.), Proceedings of the International Symposium on Acoustical Imaging, vol. 17, Plenum Press, New York, 1989, p. 219.
[7] V.B. Elings, J. Gurley, US Patent No. 5,226,801, 1993.
[8] W.F. Stockey, in: C.M. Harris, C.E. Crede (Eds.), Shock and Vibration Handbook, McGraw-Hill, New York, 1976.
[9] K.L. Johnson, Contact Mechanics, Cambridge University Press, Cambridge, 1995.
[10] D. Krüger, B. Anczykowski, H. Fuchs, Ann. Phys. 6 (1997) 341.
[11] S. Hirsekorn, Appl. Phys. A 66 (1998) S249.
[12] M. Muraoka, W. Arnold, JSME Int. J. A 44 (2001) 396.
[13] E. Kester, U. Rabe, L. Presmanes, Ph. Tailhades, W. Arnold, J. Phys. Chem. Sol. 61 (2000) 1275.
[14] Data sheet of PI Ceramic, Lindenstraße, D-07589 Lederhose, Germany.
[15] B. Jaffe, W. Cook, H. Jaffe, Piezoelectric Ceramics, Academic Press, London, 1971.
[16] G.S. Kino, Acoustic Waves: Devices, Imaging, & Analog Signal Processing, Prentice-Hall, Englewood Cliffs, NJ, 1987.
[17] V. Scherer, S. Hirsekorn, U. Rabe, W. Arnold, in: D.O. Thompson, D.E. Chimenti (Eds.), Review of Progress in QNDE, vol. 19, Plenum Press, New York, 2000, p. 1493.
[18] Q.M. Zhang, J. Zhao, K. Uchino, J. Zheng, J. Mater. Res. 12 (1997) 1493.
[19] U. Rabe, Ph.D. thesis, Technical Faculty of the University, Fraunhofer Institute for Nondestructive Testing, Saarbrücken, Germany, 1996, unpublished.
[20] L.M. Eng, H.J. Güntherodt, G.A. Schneider, U. Köpke, J. Muñoz-Saldaña, Appl. Phys. Lett. 74 (1999) 233.
[21] K. Franke, J. Besold, W. Haessler, C. Seegebarth, Surf. Sci. Lett. 302 (1994) L283.
[22] M. Labardi, V. Likodimos, M. Allegrini, Phys. Rev. B 61 (2000) 14390.